BARC/1999/E/001

BARC/1999/E/001

सत्यमेव जयते

ION ASSISTED DEPOSITION OF REFRACTORY OXIDE THIN FILM COATINGS FOR IMPROVED OPTICAL AND STRUCTURAL PROPERTIES

by

N. K. Sahoo, S. Thakur, D. Bhattacharyya and N. C. Das
Spectroscopy Division

1999

BARC/1999/E/001

GOVERNMENT OF INDIA
ATOMIC ENERGY COMMISSION

ION ASSISTED DEPOSITION OF REFRACTORY OXIDE THIN FILM COATINGS FOR IMPROVED OPTICAL AND STRUCTURAL PROPERTIES

by

N.K. Sahoo, S. Thakur, D. Bhattacharyya, and N.C. Das
Spectroscopy Division

BHABHA ATOMIC RESEARCH CENTRE
MUMBAI, INDIA
1999

BIBLIOGRAPHIC DESCRIPTION SHEET FOR TECHNICAL REPORT
(as per IS : 9400 - 1980)

01	*Security classification :*	Unclassified
02	*Distribution :*	External
03	*Report status :*	New
04	*Series :*	BARC External
05	*Report type :*	Technical Report
06	*Report No. :*	BARC/1999/E/001
07	*Part No. or Volume No. :B*	
08	*Contract No. :*	
10	*Title and subtitle :*	Ion assisted deposition of refractory oxide thin film coatings for improved optical and structural properties
11	*Collation :*	39 p., 32 figs.
13	*Project No. :*	
20	*Personal author(s) :*	N.K.Sahoo; S. Thakur; D. Bhattacharyya; N.C. Das
21	*Affiliation of author(s) :*	Spectroscopy Division, Bhabha Atomic Research Centre, Mumbai
22	*Corporate author(s) :*	Bhabha Atomic Research Centre, Mumbai - 400 085
23	*Originating unit :*	Spectroscopy Division, BARC, Mumbai
24	*Sponsor(s) Name :*	Department of Atomic Energy
	Type :	Government

Contd... (ii)

30	*Date of submission :*	February 1999
31	*Publication/Issue date :*	March 1999
40	*Publisher/Distributor :*	Head, Library and Information Services Division, Bhabha Atomic Research Centre, Mumbai
42	*Form of distribution :*	Hard Copy
50	*Language of text :*	English
51	*Language of summary :*	English
52	*No. of references :*	32 refs.
53	*Gives data on :*	

60 *Abstract* : Ion assisted deposition technique (IAD) has emerged as a powerful tool to control the optical and structural properties of thin film coatings. Keeping in view the complexity of the interaction of ions with the films being deposited, sophisticated ion sources have been developed that cater to the need of modern optical coatings with stringent spectral and environmental specifications. In the present work, the results of ion assisted deposition (IAD) of two commonly used refractory oxides, namely TiO_2 and ZrO_2, using cold cathode ion source (CC-102R) are presented. Through successive feedback and calibration techniques, various ion beams as well as deposition parameters have been optimized to achieve the best optical and structural film properties in the prevalent deposition geometry of the coating system. It has been possible to eliminate the unwanted optical and structural inhomogeneities from these films using an optimized set of process parameters. Interference modulated spectrophotometric and phase modulated ellipsometric techniques have been very successfully utilized to analyze the optical and structural parameters of the films. Several precision multilayer coatings have been developed and are being used for laser and spectroscopic applications.

70	*Keywords/Descriptors :*	TITANIUM OXIDES; ZIRCONIUM OXIDES; SURFACE COATING; THIN FILMS; SPUTTERING; GRAIN SIZE; ELLIPSOMETRY; PRESSURE DEPENDENCE; OXYGEN; FLOWSHEETS; CURRENT DENSITY; TEMPERATURE DEPENDENCE; OPTICAL PROPERTIES; ELECTRON BEAMS
71	*INIS Subject Category No. :*	B2310
99	*Supplementary elements :*	

Ion Assisted Deposition of Refractory Oxide Thin Film Coatings for Improved Optical and Structural Properties

ABSTRACT

Ion assisted deposition technique (IAD) has emerged as a powerful tool to control the optical and structural properties of thin film coatings. Keeping in view the complexity of the interaction of ions with the films being deposited, sophisticated ion sources have been developed that cater to the need of modern optical coatings with stringent spectral and environmental specifications. In the present work, the results of ion assisted deposition (IAD) of two commonly used refractory oxides, namely TiO_2 and ZrO_2, using cold cathode ion source (CC-102R) are presented. Through successive feedback and calibration techniques, various ion beams as well as deposition parameters have been optimized to achieve the best optical and structural film properties in the prevalent deposition geometry of the coating system. It has been possible to eliminate the unwanted optical and structural inhomogeneities from these films using an optimized set of process parameters. Interference modulated Spectrophotometric and phase modulated Ellipsometric techniques have been very successfully utilized to analyze the optical and structural parameters of the films. Several precision multilayer coatings have been developed and are being used for laser and spectroscopic applications.

Ion Assisted Deposition of Refractory Oxide Thin Film Coatings for Improved Optical and Structural Properties

1. Introduction

Post-deposition instabilities in optical and mechanical properties of optical coatings are the major concern for developing precision thin film device [1]. The cause of this undesirable behavior is the strong tendencies of the films to develop columnar microstructure during the physical vapor deposition (PVD) process [2]. One of the possible approaches to eliminate such a growth condition is to provide more kinetic energy to the vapor molecules. This leads to greater mobility during the condensation process thereby leading to higher packing density. Over the years, it has been realized that such improved and favourable properties can be obtained by bombarding the growing films with high energetic oxygen, argon or any other suitable ions or combination of ions (Fig.1) [3]. Such techniques are popularly known as ion assisted deposition (IAD) techniques (Fig.2). It has been consistently observed that enhancement of ionization in sputtering and introduction of ions in evaporation not only improve the situation but also offer a large number of variables for the control of film properties.

These processes have been subjected to some excellent reviews in the past [4-7], which have provided a larger insight into the mechanism of the fundamental process. But till now, the experimental studies, theory and modeling differ from each other on various aspects such as,

a). Process or technique of generating the ions,

b). Control and distribution of ion energy and current densities,

c). Associated deposition parameters

and

d). Ion beam neutralization.

Inspite of the differences in the approaches, almost all IAD related studies report improvement of film properties under optimized conditions. The IAD process over the years has revolutionized the entire field of optical thin films apart from a host of other

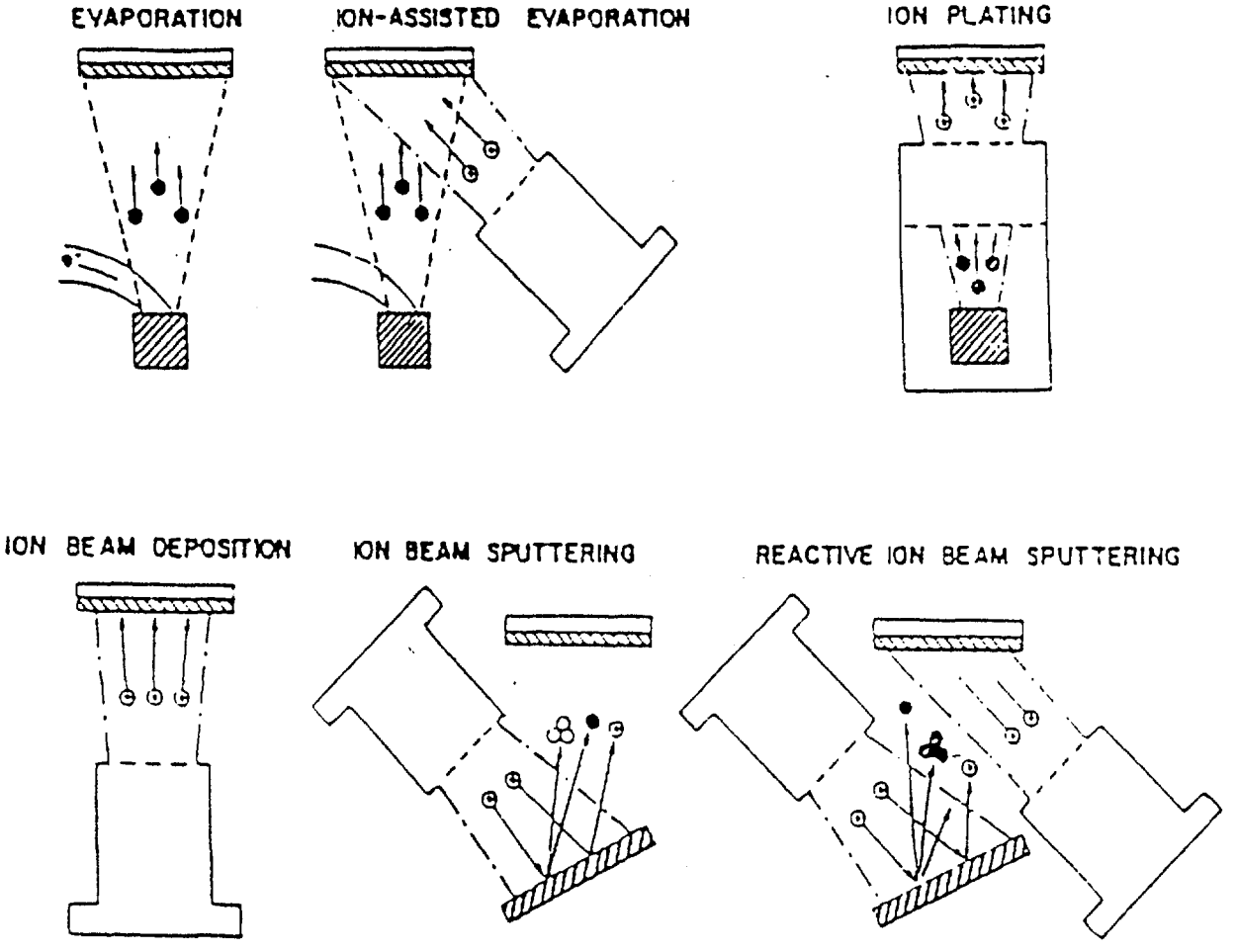

Fig1. Schematic of Deposition Processes utilizing ions

related fields and has enabled the experimentalist to achieve properties, which was considered impossible.

2. Effect of Ion beam bombardment on thin film properties

The interaction of energetic ions with solid surfaces has been studied extensively because of its importance in many high technology processes such as plasma wall effects in fusion research, ion etching in device manufacture and ion-beam analytical techniques. The energy range of importance in IAD is from thermal energies up to about 1 keV. Carter and Armour have identified the following four physical processes as the most important ion-based film process in this energy regime [4].

(1) Desorption or sputtering of impurities from the substrate surface by ion impact.

(2) Penetration and entrapment of coating and support gas in the growing film.

(3) Sputtering of the substrate and eventually the coating as film growth progresses.

(4) The generation of defects in the substrate and the growing film.

Some of the growth models are currently in use to explain the effect of ion beams on properties of thin films. One of the first models developed similar to the ion assisted process was the thermal spike model by Muller [5]. In this model, the ion beam was assumed to create temperature spikes due to ion penetrating just below the surface of the films. This induced an atomic reordering in the porous dielectric network of the growing film. It has been computed that during the spike life time, which was around 10^{-11} seconds, atomic reordering of the surface atoms took place at a rate which was proportional to the mass of the film species, the lattice spacing and a local activation energy. At an ion to atom arrival ratio one, it results in the disruption of the micro columnar growth and bridging develops, causing the closure of the voids. Another model developed by Brett has simulated the ion bombardment effect on the structural properties of the films [7]. It was found, from this simulation, that an ion to atom arrival ratio of one, the packing density of the films increased only slightly from 0.61 to 0.66. The microcolumns, at this point, became less defined and bridging and branching suppressed the continuous voids. A subsequent model developed by Muller explains that more or less the mechanism is associated with the ion-induced densification [6]. As per this model, when ions with energy of a few hundred electron volts strike the surface of a porous film, they penetrate to a maximum depth of a few interatomic spacings. The

interacting ions produce phonons, vacancies, knock-on atoms and electronic excitations. The ions are either back-scattered or incorporated, while knock-on atoms may leave the surfaces as sputtered atoms or penetrate deeper into the film where they get trapped as interstitials. Vacancies near the surface, which are caused by bombarding ions, are partially refilled by the newly arriving vapour atoms. For a sufficiently large ion to vapour atom arrival ratio, the latter mechanism will result in downward packing of the material, such that films no longer grow in porous columnar microstructures but instead grow in densely packed structures. Muller has subsequently refined this model using molecular dynamics approach wherein the film growth is described as the evolution of a representative sample of a many body atomic system in time and space by fully allowing for mutual atomic interactions [7].

Studies of influence of mono-energetic ion bombardment on the nucleation of thin film by Dobrev and Marinov showed that in case of 1-10 keV argon ion on silver, gold, cadmium and cobalt surface mobility of adatoms was increased and nucleation was accelerated [8]. Similar observations were made by Babnev et al for Ar and Ne ion-assisted deposition of Zn on CuO_2 and Sb on NaCl [9]. In general the effects of ion irradiation is to create activation sites that simulates nucleation and develop nucleation orientation. A significant increase in crystalline perfection of a film can be achieved if self-ion bombardment is present, i.e., through partial ionization of the evaporant flux, and is a promising method for epitaxial growth. Ion assisted deposition has been shown to modify the stress in growing films. Germanium films have been deposited reduced stress under critical ion densities and the stress in niobium films changed from tensile to compressive under high argon ion bombardment fluxes.

The development of columnar microstructure during film growth has been simulated in two and three dimensions by various computer models as shown in Fig.3. A recent calculation by Muller shows that heating the substrate during growth can reduce the void density. The improvement in film packing density with substrate temperature has been investigated experimentally for a range of dielectric materials. The packing density for some materials is however still less than unity at 300 °C. The more satisfactory approach is to add activation energy to the growing film in order to disrupt the columnar growth without heating the substrate.

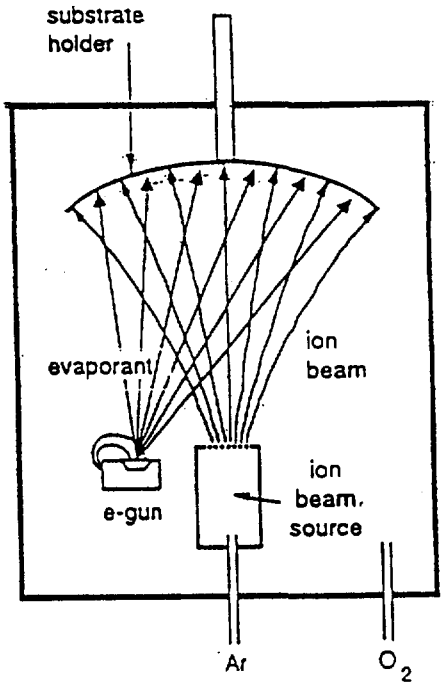

Fig.2 Schematic of ion-assisted deposition in PVD process using electron beam gun

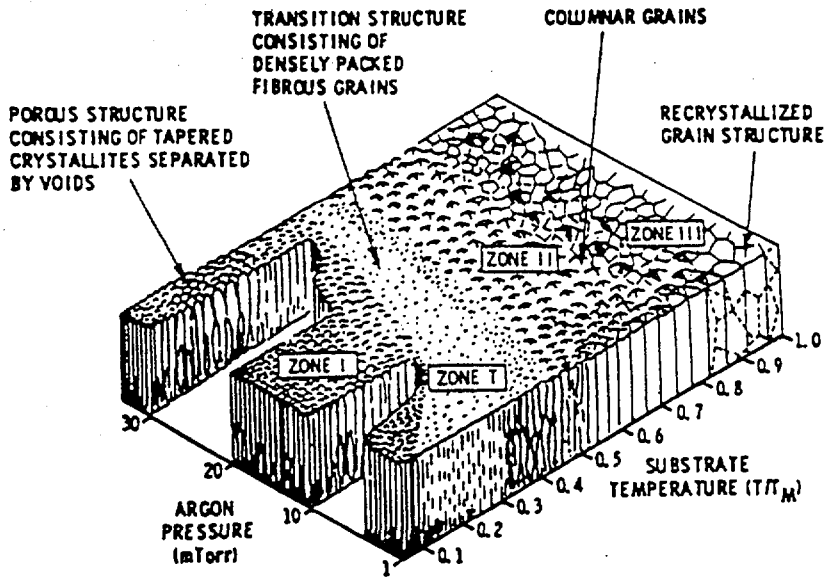

Fig.3 The three dimensional zone structure model showing the relationship between the thin film microstructure, substrate temperature and pressure during film deposition process.

In general, oxygen ions rather than inert gas ions are required to reduce and compensate for any preferential sputtering of oxygen atoms from dielectric oxide films. However, some successful results also have also been achieved with oxygen-assisted deposition of MgF_2 and Na_3AlF_6 (cryolite) [10]. Very interesting observations of abrupt reduction of interfacial refractive index have been reported, when non-IAD layer is deposited on a densely packed IAD layer. It is reported that when ZrO_2 vapour is deposited onto an ion-assisted dense ZrO_2 layer, the film instantaneously grows in the form of a porous network. Previous studies have also indicated that the refractive index increases and reaches a plateau when the columnar microstructure is eliminated.

2.1 Grain Size

Various researchers have reported on the effect of ion bombardment on the grain sizes of metal films. In most cases ion bombardment resulted in a decrease in grain size with increasing energy. No such systemized data is available for dielectric and semiconductor films. However on the basis of limited published data the following conclusions can be made. For lower level of ion bombardment the films generally amorphous. CeO_2 films are crystalline at all energies where as TiO_2, Ta_2O_5, ZrO_2 and silica films are amorphous at low energies and ion fluxes [11-14]. The formation of cubic phase of zirconia on heated substrates indicates a small grain size in these films. Ta_2O_5 films on heated substrates in the presence of ions are crystalline where as on unheated substrates up to 500 eV energy and 45 $\mu A/cm^2$ ion current density are amorphous. The films at 90 mA/cm^2 were crystalline but this has been attributed recrystallization into a reduced oxide at higher flux. None of the films showed any preferred orientation and had to be post deposition annealed to achieve crystallinity.

2.2 Density

One consequence of the decrease in grain sizes on ion bombardment is the increased density. By the molecular dynamics approach, this would mean elimination of columnar microstructures resulting in less porous films which are less susceptible to environmental changes over a period of time. Most importantly, the refractive index would approach that of the bulk material with increase in density. In a study made by

Martin et al, it was found that the film density as measured using a quartz microbalance, increased with increase fluxes. This can be directly correlated with the refractive index behaviour of their films [15,16].

2.3 Stress

The intrinsic stress in ion bombarded films are of considerable interest for various applications. In metal films it has been observed that up to a certain flux the stresses decrease to a minimum value showing an increase beyond the optimum and finally relaxation is observed. However, Mcnil et al didn't find any changes in the stress for their silica films. In dual IBSD films of zirconia the compressive stress reduced with increase in ion flux of the secondary ion beam [17].

3 Effect of Preferential Sputtering during IAD

Almost all-dielectric oxide coatings show degradation in optical properties beyond a certain energy and ion flux. This behaviour is attributed to phenomena called preferential sputtering of oxygen at high ion fluxes and energies. In this process, the oxygen is preferentially sputtered from the growing film causing a degradation of stoichiometry. Various reasons have been attributed to this behaviour but the most reasonable one seems to be one postulated by McNally based on a model proposed by Winters and Sigmund [18]. He has modeled the incident ion as transferring its kinetic energy in a series of collisions with the lattice atoms. The collisions are assumed to be independent binary events between a moving particle, i.e., the incident ion and the lattice atoms at rest. For elastic collisions, the energy is not actually distributed amongst the different mass atoms in the solid. To evaluate this criterion an energy transfer factor (γ) for each binary collision must be calculated. The energy transfer factors are given by

$$\gamma = 4M_1M_2/(M_1 + M_2)^2 \qquad \ldots(1)$$

where M_1 and M_2 are the masses of the colliding atoms. For his study on Ta_2O_5, Al_2O_3, and silica films he calculated the following values

$$\gamma_{o-o} = 1.000,\ \gamma_{o-Ta} = 0.298$$

$$\gamma_{o-Al} = 0.935,\ \gamma_{o-Si} = 0.926$$

The γ value for Al and silica are very close to one in an almost equal energy distribution. This reduces the probability of preferential sputtering of oxygen from these compounds. Correspondingly, the large difference in atomic masses of T_a and O results in a more efficient energy deposition due to the oxygen atoms $g_{o\text{-}o} > g_{o\text{-}Ta}$ and hence in a higher probability of sputtering oxygen from tantalum. It was observed that the above calculations showed excellent agreement with the experimental results indicating that a binary collision mechanism is the most probable mechanism for this process. It also significantly matches with the molecular dynamics approach of Muller. Targove et al have subsequently published some direct experimental evidence for this momentum transfer mechanism by using three different gases for IAD of LaF_3, viz Ar, Kr and Xe at 500 eV[7]. Due to the difference in atomic masses a fixed energy would mean different momentum for three species. Using first thermal spike model they assumed at a constant energy the number of atoms arranged during a spike n_T to be proportional to the ion current density, *J*. This did not give linear fit to the results. However, on assuming a momentum transfer mechanism, the rate of momentum transfer P_{tot} was approximated as follows.

$$P_{tot}=J.(2m.\gamma.E)^{1/2} \qquad ...(2)$$

Where E is the ion energy, m is the ion mass and γ is the energy transfer criterion as per the previous discussion. This relation was found to give an excellent fit to the experimental values suggesting that increase in index and packing density is momentum related, supporting Muller's model. Kao and Gorman's work on dual ISBD zirconia films is also significant in this direction. They have found that the effect of the secondary ion beam is much more pronounced than that of the heating the substrates even at low ion fluxes, indicating again a momentum transfer kind of mechanism.

4. Various types of Ion sources

Over the years a number of ion gun geometries have been experimented for IAD applications (Fig.4-8). Most of the significant ion assisted deposition (IAD) work so far has been done with the Kaufman type ion source [19]. This commonly used ion source is complicated but well reputed, The ion energy and its distribution are well defined due to independent control of the plasma generation and the ion extraction (Fig.5). But the

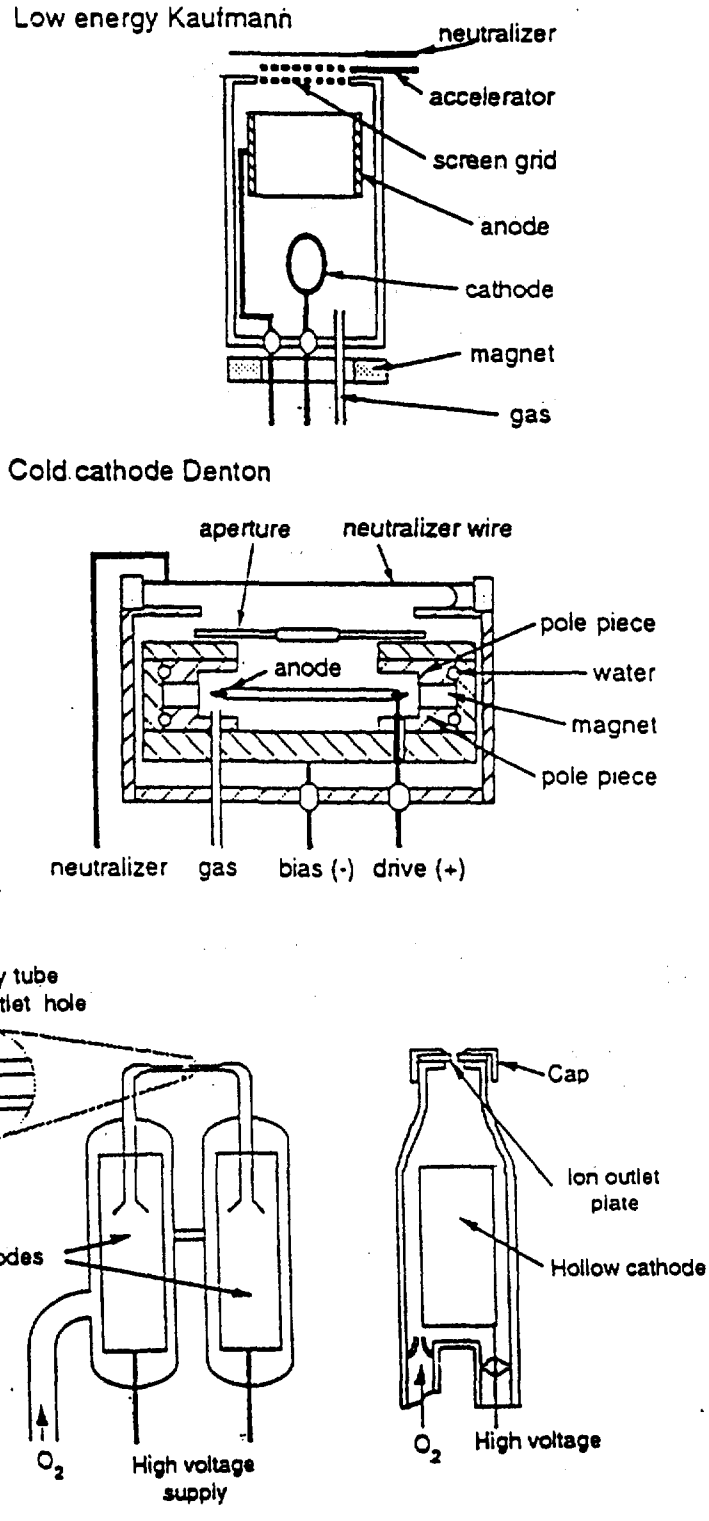

Fig.4 Schematic of Low Energy Kaufmann, Cold Cathode Denton, Heitmann and Ebert Ion Sources

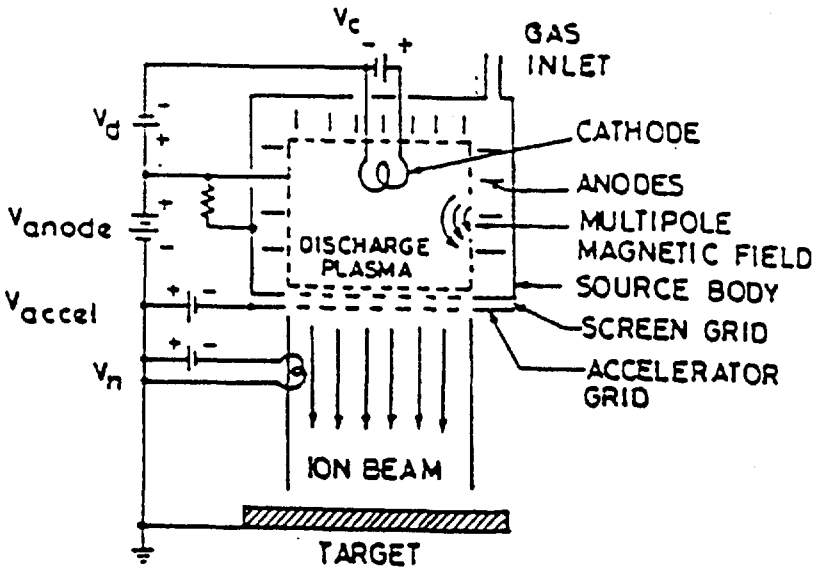

Fig. 5 Schematic of a broad beam multi aperture Kaufman source

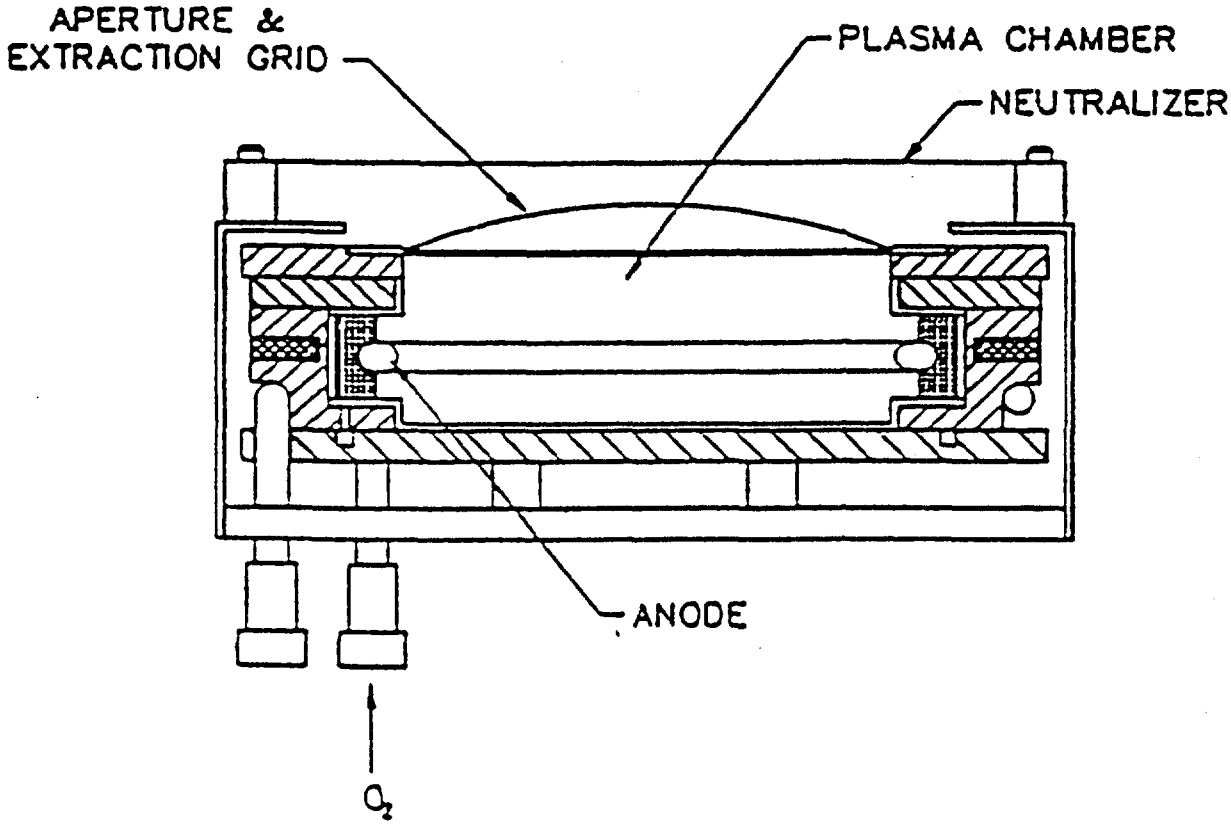

Fig.6. Schematic of ion source used in the present study

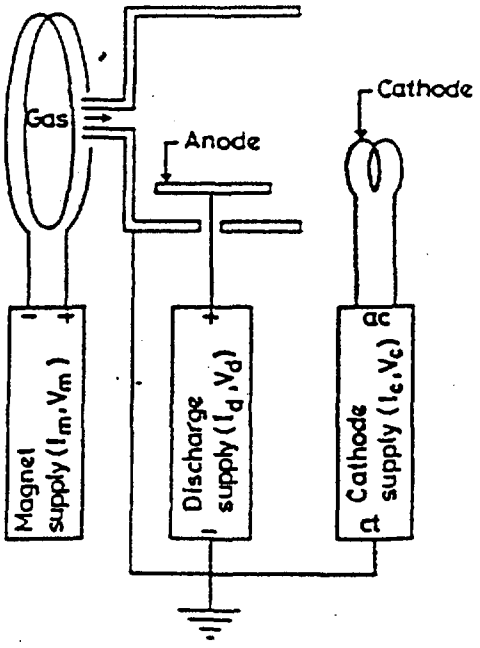

Fig.7 Schematic of the end Hall type of ion source

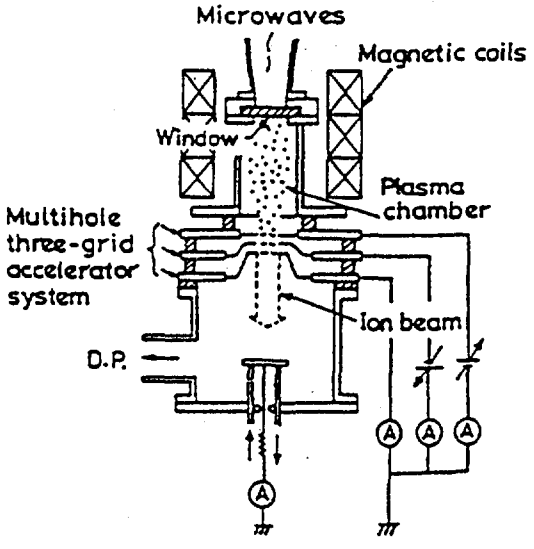

Fig.8 Schematic of microwave ion source

primary limitation of such type ion source is the energy distribution, which is very much similar to that of a laser beam. Some early IAD work has been done with the Heitman and Ebert type ion sources, from which ions are extracted from the glow discharge generated in a hollow cathode as shown in Fig.4 [20]. A low energy and high current ion source that recently developed for IAD application is known as End-Hall type ion source (Fig.7) [21]. It is easier to maintain this source as it is grid less. The cathode is positioned in front of the anode and an axial magnetic field traps the electron. Although the ion energy is low, 50-100eV, the ion current can be as high as 1A. There are also microwave ion sources (Fig.8), which are used with reactive plasma etching applications. The ion source used in the present studies is a magnetron type cold cathode ion source (Fig. 6) [22]. Because the effects on ion bombardment depend very much on the quality of the beam such as flux, energy, and their distributions, it cannot be taken for granted that the beneficial effects achieved with one ion source cannot be obtained with another.

5. Effect of Energy Distribution of the Ion Beam

The collective behaviour of ions is as important as the effective energy of the beam. That's why, besides the beam energy, the energy distribution of the ions is a key factor in getting the improved film properties. For a Kaufman source, its energy spread reported to be very narrow, i.e., ΔE=1 to 10eV [23]. For cold cathode discharge source, the energy spread is around 10-50eV (Fig.9) [24]. The energy spread of the later presumably can be much wider if a source is designed with very effective electron trapping, so that it can operate at a low pressures with reasonable voltage (e.g., <1500eV). In that case, the discharge relies heavily on multiple ionization to sustain the plasma without thermionic support. An ionizing electron, after making several ionization collisions, could have spent a large portion of its energy before making a final ionizing impact. These finally generated ions can thus require the limited residual energy from the electron. Hence, the ions extracted from such a plasma source, e.g., plasma generated in the ion source used in the present studies, could indeed have a low energy and large energy spread due to multiple ionization. This is clearly very different from the ions generated from the Kaufman source. Figure-9 illustrates the difference; the

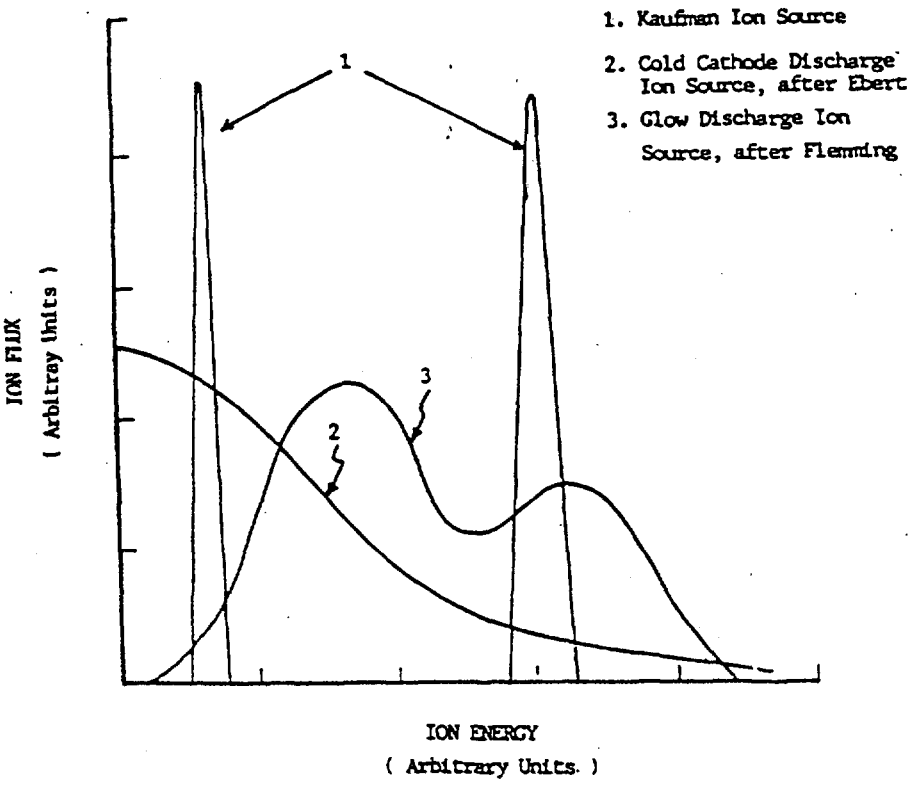

Fig.9 Energy Distribution of ions produced by various ion sources

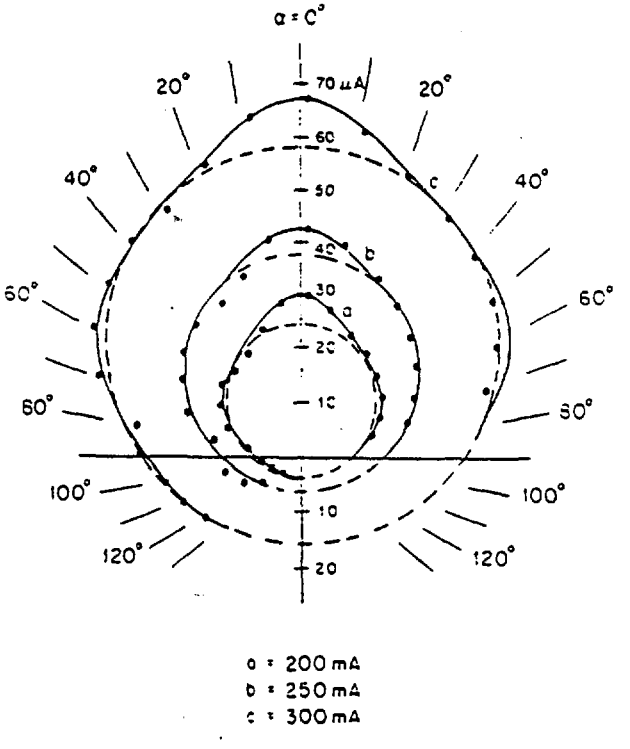

Fig.10 Experimental measurement of angular variation of ion current density for coid cathode ion source equipped with a 32-mm dia. aperture [25]

Kaufman ion beam resembles a laser beam, and the cold cathode sources white radiation (Fig10). In most cases, an ion source of well-defined energy is superior in terms of better process control, e.g., focusing and mass separation. However, there are also situations where a broad distribution of energy is beneficial, as reported in this study.

6. Mechanism of Densification

The mechanism of densification by ion-assisted deposition can be largely understood in terms of ion-atom and atom-atom collisions on the growing films. An ion with energy

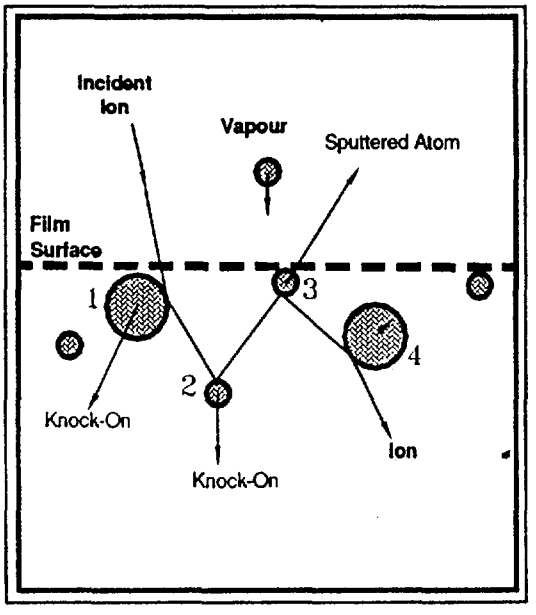

Fig.11 Simplified IAD model to explain the generation of vacancies in the near surface region by ion impact.

up to 1 keV can penetrate the surface of a material to an average depth of a few nanometers and produces a collision cascade of knock-on atoms. The displacement of target atoms results in the formation of vacancies close to the surface of the film and forward recoiled atoms pushed into interstitial sites deeper in the materials. The effect is

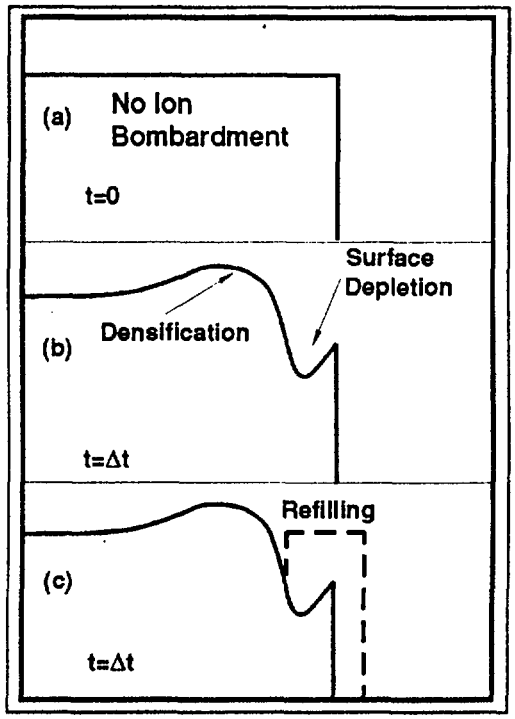

Fig.12 Surface depletion by ion impact and subsequent refilling by atoms from the vapour stream

to deplete the surface atoms and densify the film at greater depths (Figs.11 & 12). The depleted area then is partially replenished by arriving atoms from the vapour stream and the process repeated. Computer simulations based on modification of a three dimensional cascade calculation are reported to be in excellent agreement with the experimental data. From the deposition geometry and ion gun parameters, it is possible to calculate the spatial distribution of average ion-beam current densities for stationary as well as rotating substrate. It can be shown that the average ion current density I(r) is given by the expression [25]:

$$I(r) = \frac{h^2 c}{N} \sum_{i=1}^{N} \frac{F(\alpha_i)}{\left(c^2 + d^2 + r^2 - 2dr\cos\beta_i\right)^{3/2}} \quad \ldots(3$$

Where,

$$\alpha = \cos^{-1}\left[\frac{c^2 + d^2 + r(e-d)\cos\beta - de}{\sqrt{(c^2 + d^2 + e^2 - 2de)}.\sqrt{(d^2 + c^2 + r^2 - 2dr\cos\beta)}}\right] \quad \ldots(4)$$

The angles and distances are defined in Fig.13. It is observed that the quantity F(α) depends somewhat upon the total pressure in the system and on the location with regard to the walls of the chamber.

7. Experimental

In the present study, the ion bombardment is provided by a Denton's CC-102R cold cathode ion source whose ion current density profile and I-V characteristics are shown in Figs. 14 and 15. The arrangement used for our experiments is shown in Fig.13. The coating system is a fully automated VERA-902 box coater equipped with electron beam guns, resistance sources, quartz crystal monitors, optical monitor, substrate heater, substrate rotation mechanism and mass flow controllers as shown in Fig. 16. All the component modules have been interfaced with Siemens process controller. Details of the functional cross section of the ion gun are depicted in Fig.6. The ring anode and C-shape circular magnetic pole pieces produce the closed E X B loop in the source cavity, which acts as an electron trap for efficient impact ionization. With application of a positive potential to the anode and admission of gases (Ar, O_2, etc.) into the cavity, a plasma of the support gas is generated. Ions are extracted from the plasma with various extraction apertures located on the top opening of the source body. The current-voltage characteristics and beam profiles of the source operating with the extraction aperture B is shown in Fig. 14 and 15. In our experiment we have mainly used aperture B which is a dome shaped Al wire screen having a transparencies of 65% and a 11 cm of radius of curvature. With this aperture it is possible to operate the source at chamber pressures of 1 - 4×10^{-4} mbar in a system with ~3000 l/s effective pumping speed. The total beam current is measured as the difference between source current and cathode return current. For the above aperture B, the beam current is fairly constant at 15% of the source current. Typical operating source voltage range from 400 to 1200V. The placement of ion source allowed the arrival of ions at the substrate surface with a 20° angle of incidence, from a distance of 35 cm.

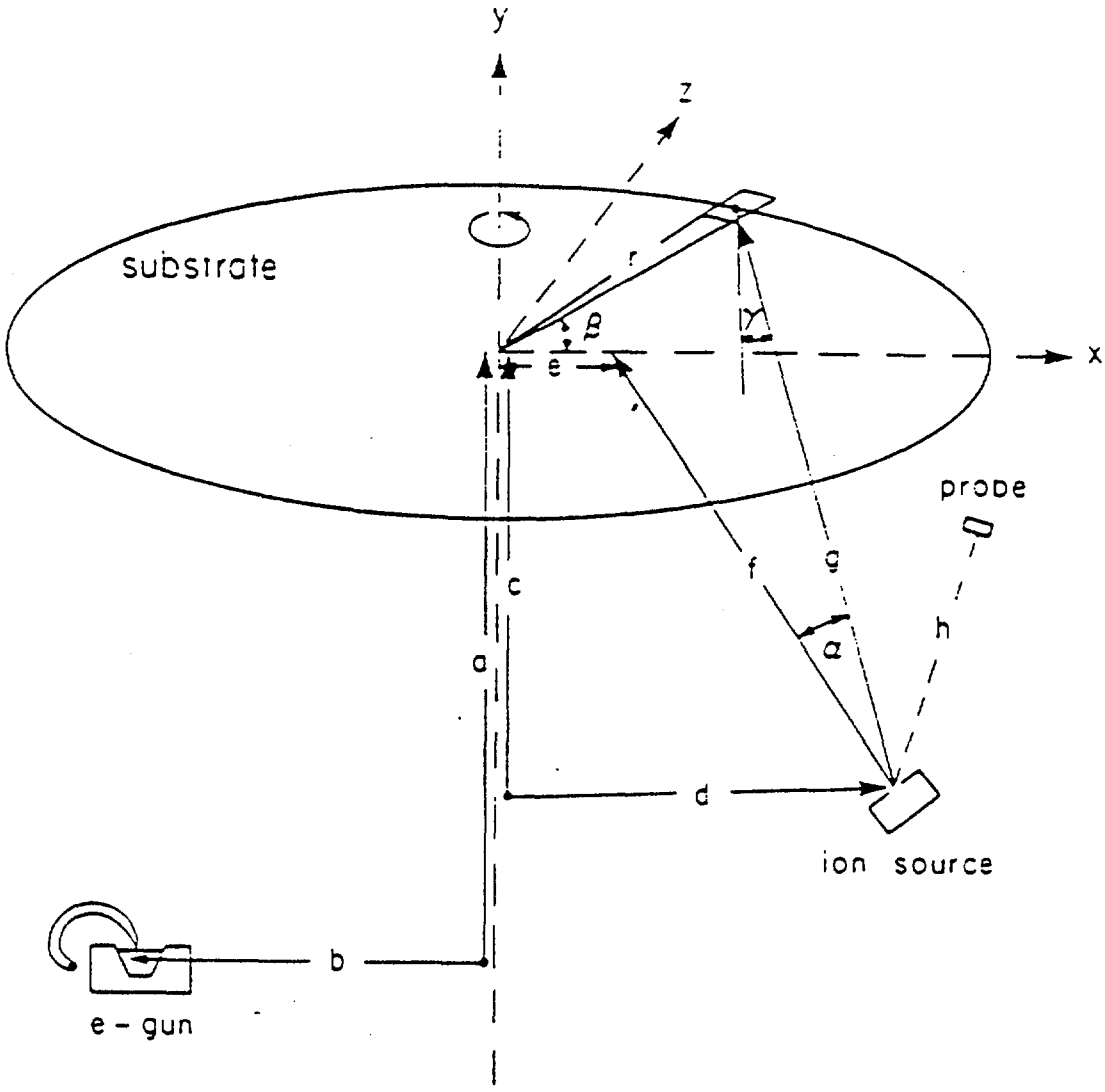

Fig.13 Position of electron beam gun and ion gun in the deposition chamber and various parameters used in equations 3 & 4.

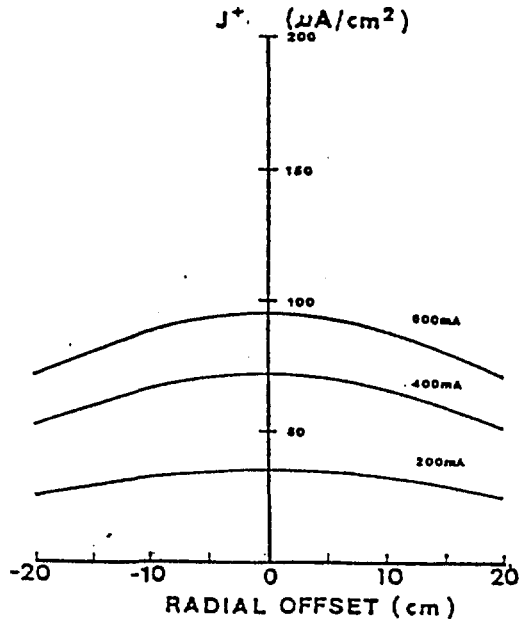

Fig.14 Ion density profiles of CC102R ion source measured at 55 cm above source aperture, operating at 1.x10⁻⁴ torr of O_2 and various source currents with Aperture B. (Courtesy: Denton's user manual for CC102R)

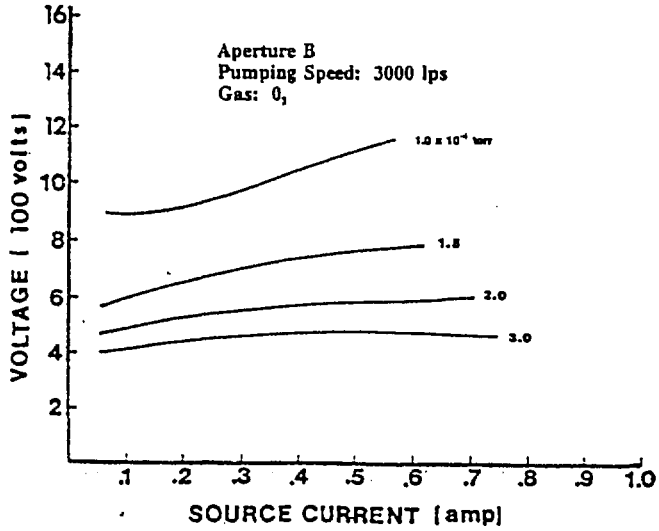

Fig.15 I-V Characteristics of CC-102R ion source, operating with Aperture B at various chamber pressure (Courtesy: Denton's user manual for CC102R)

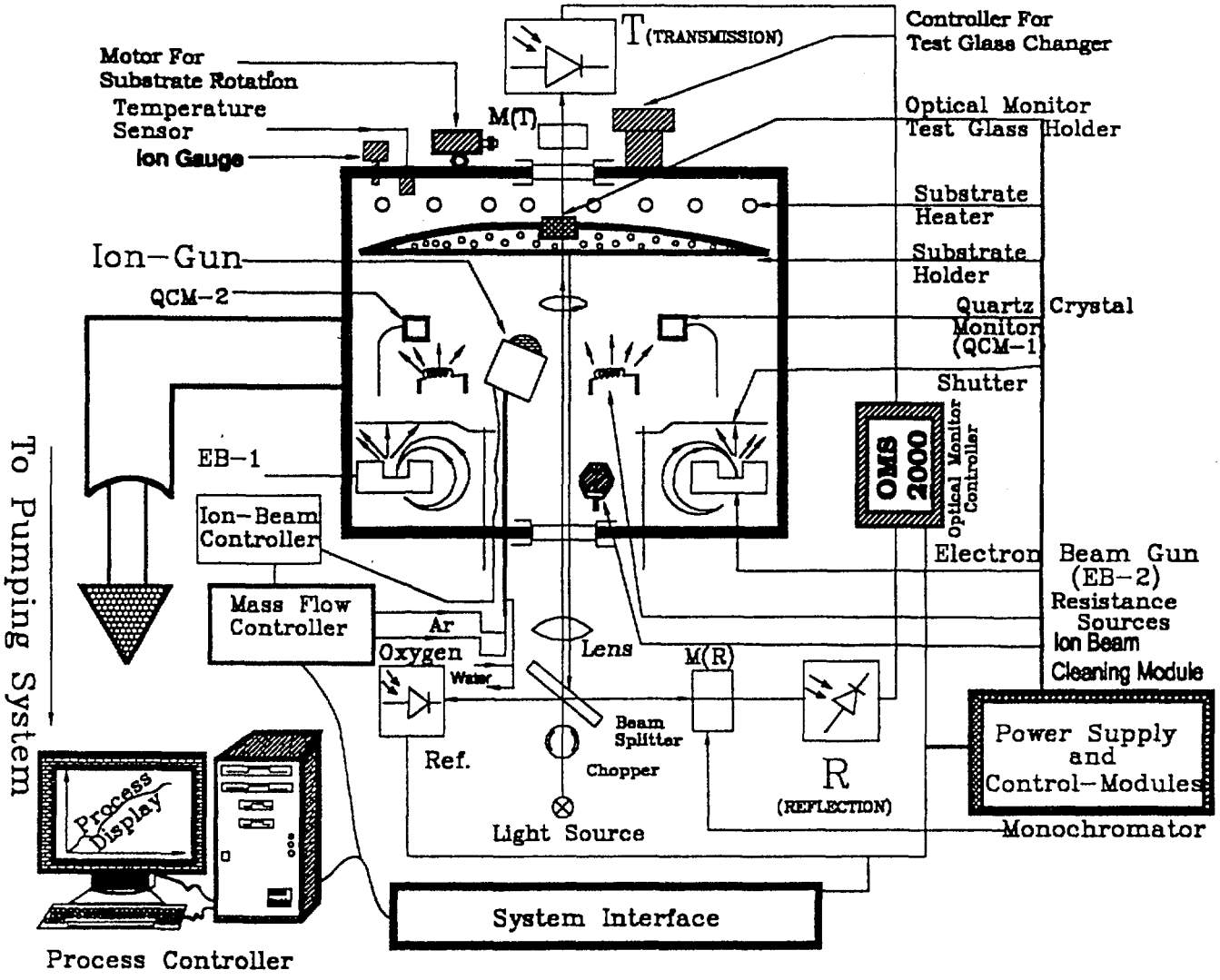

Fig.16 Schematic of VERA 902 optical coating system equipped with Ion Gun and co-deposition facilities

7.1 Effect of Substrate Temperature during IAD process

We have observed that the ion beam has a very prominent effect when the substrate temperature is kept at a medium or low temperature (<200 °C). But at higher substrate temperatures (>300 °C) the improvement can be observed with very high ion current densities. According to a model proposed by Movchan and Demchishin, the important parameter determining the microstructure of metal and dielectric thin films is the ratio of the substrate temperature (T_s) and the melting point of the evaporant (T_m) [26]. For $T_s/T_m < 0.45$ the film microstructure is mostly columnar. Thornton later modified this model to include the effect of pressure in the sputtered coatings. He proposed a T_s/T_m value of 0.3 or less for the columnar growth. This growth has been confirmed from electron microscopic observations of cross sections of thin films [27]. One important consequence of a columnar growth is the loosely packed nature of the film causing moisture absorption and hence columns exerting mutual force of attraction causing stress. The columnar growth also results in the birefringence which in turn results in an anisotropic refractive index with the index along the direction of columns being higher than the along the plane of the substrates. On Ar^+ irradiated Ni film it is observed that a low j_i/j_a value resulted in the closure of open voids with a large ion fluxes resulted in total collapse in the microporous structure. Here j_i is the ion arrival rate and j_a is the vapour arrival rate. Muller et al has also modeled this hypothesis on IAD zirconia films[7]. It is also reported that on ceria films by Muller that beyond a certain energy for $J_i/j_a = 1$ the density starts decreasing. This has been attributed to a decrease in surface vacancy cross section at higher enrgies. Hirsch and Varga and Brighten and Huebler later defined a critical ion atom arrival rate ratio beyond which a stress annealing took place[7]. While Hirsch and Varga have defined a dependence of the kind:

$$\left[\frac{j_i}{j_a}\right]_c = kE^{3/2} \qquad \ldots(5)$$

Where E is the incident energy, k is a constant(1-10), j_i is ion flux and j_a is atom flux. Brighton and Hubler defined a relation of this kind:

$$\left[\frac{j_i}{j_a}\right]_c = \left(\frac{1}{NV}\right) \qquad \ldots(6)$$

Where N is the film atomic number density and V is the average volume of collision cascade.

Hirsch and Varga [28] assumed a thermal spike to result in this annealing while Brighton and Hubler [29] attribute this to the collision cascade caused by knock on atoms. Extending this concept, Grigorov et al have defined an optimum ion flux $[j_I]_{opt}$ at which the film grows with the highest degree of order and packing density [30]. If one atomic displacement per condensing particle takes place during the ion assisted growth process, then

$$[j_i]_{opt} = \left(\frac{1}{N_D}\right) j_a \qquad \ldots(7)$$

Where N_D is the average number of displacement generated by one ion. J_I is the fraction of incident particles not sputtered. Bradley et al have attempted to study theoretically the development of orientational order in thin films grown at an off normal incidence. They assumed that orientation would result from a difference in sputtering yields of the grains, which are oriented, which channel the ion beam, and those, which are not. The degree of orientational order was found to increase with ion flux and saturate beyond a certain value.

7.2 Optical and Structural Inhomogeneity

Inhomogeneities in optical and structural properties in conventional thin films had added several constraints to design precision filters and coatings [31]. The IAD has a very big advantage of generating homogeneous film even under regular process parameters. We have several instances in this present work where homogeneous conditions were very conveniently achieved with IAD technique.

7.3 Optical Properties

We have studied two very important refractory oxides, TiO_2 and ZrO_2 for our ion-assisted experiments. One of the very important properties, which govern the coating performance, is the refractive index and packing density. Depending on the deposition parameters and ion beam parameters the optical and structural properties can be improved or deteriorated. We have used two different techniques to characterize

the films to identify such effects. The one is spectrophotometric technique and the other is Phase-modulated ellipsometric technique.

7.4 Spectrophotometric Characterization

In the present investigations, the transmittance spectra of the films and the substrates have been recorded in Varian Model 2300 uv-vis-nir spectrophotometer. The instrument has the wavelength accuracy of ±0.2nm in the visible region and ±0.8 nm in the near infrared.

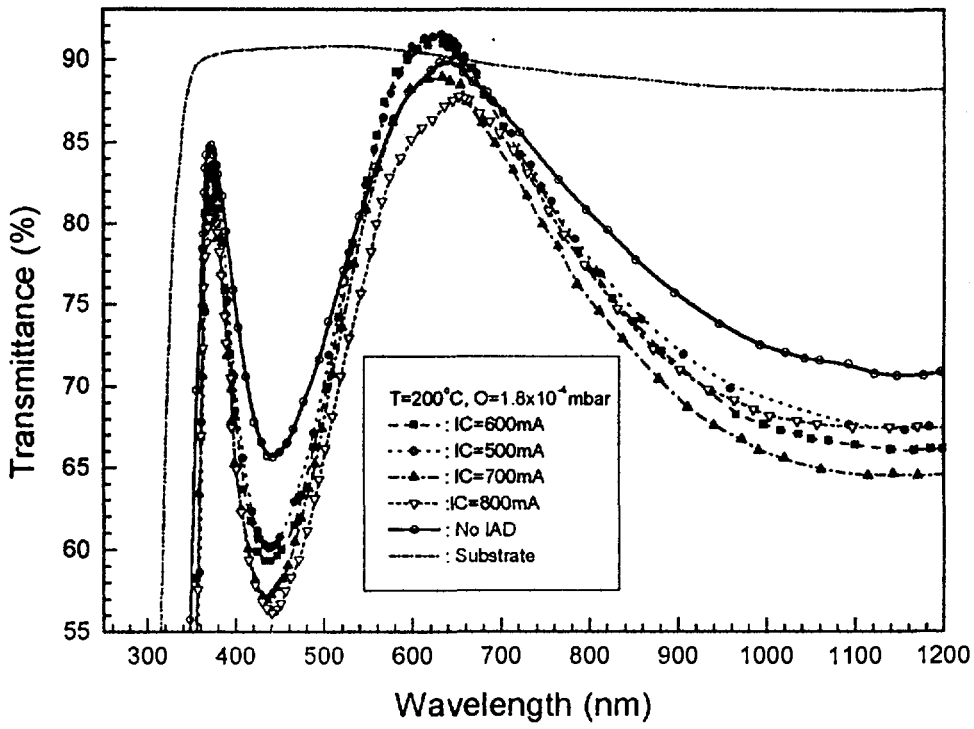

Fig.17 Interference modulated transmittance spectra of the TiO_2 films deposited under varying ion current but with same oxygen pressure and substrate temperature.

The transmittance spectra of a thin film get interference modulated and the amplitude of the modulation is a function of the refractive index, extinction coefficient and physical thickness of the sample (Figs17-20). Closer looks to such transmittance spectra reveal that the peak minima are a very strong function of the optical constants where as peak maxima is controlled by the inhomogeneity in the structure. One of the very important

observations during this experiment is relationship between substrate temperature and ion current.

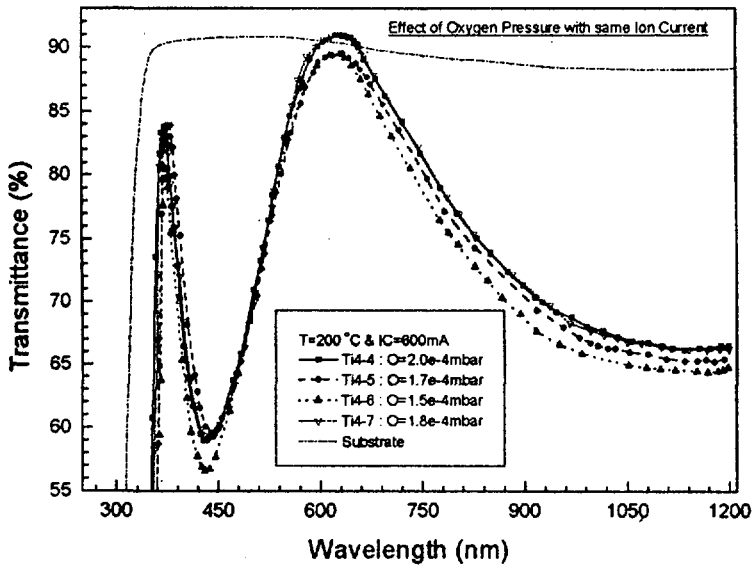

Fig.18 Interference modulated transmittance spectra of the TiO_2 films deposited under same Temperature and Ion current but with varying oxygen pressure.

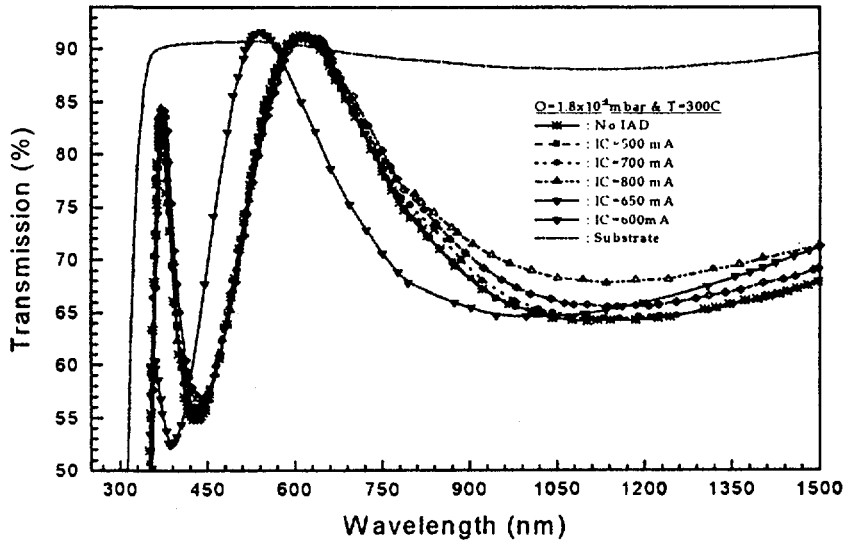

Fig.19 Interference modulated transmittance spectra of the TiO_2 films deposited under varying ion current but with same oxygen pressure and higher substrate temperature (300°C).

The improvement in optical properties of ion-assisted films is more prominent at lower temperature. As the temperature becomes high the improvement in the optical properties become very marginal.

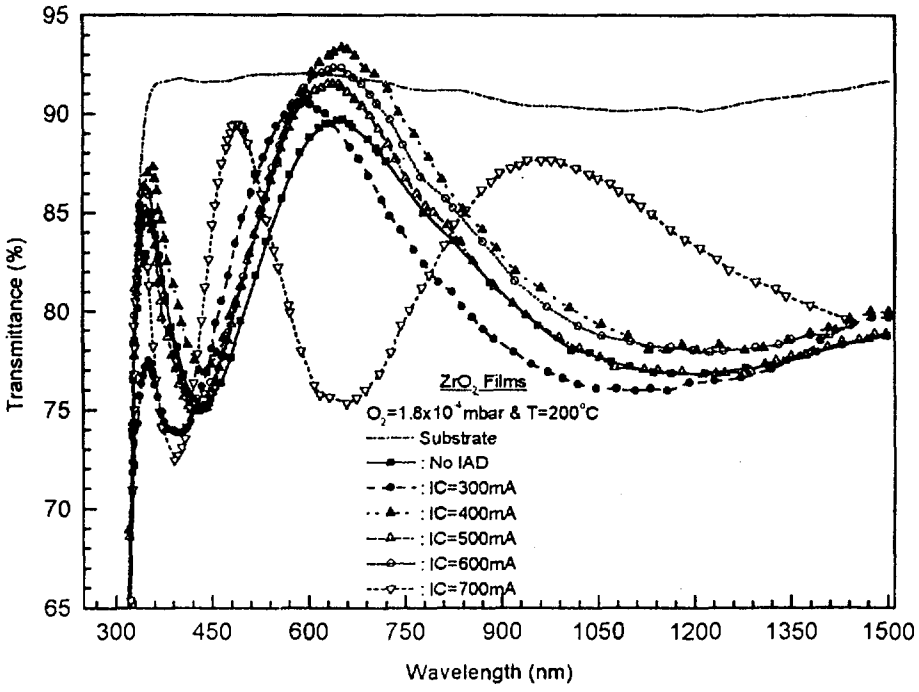

Fig.20 Interference modulated transmittance spectra of the ZrO_2 films deposited under varying ion current but with same oxygen pressure and higher substrate temperature (200°C).

As it can be seen from the transmittance plot (Fig.18), although the refractive index is highest at 1.5×10^{-4} mbar, the positive inhomogeneity is also very dominant. The film has a near homogeneous structure when the oxygen pressure was maintained at 1.8×10^{-4} mbar. With this value of optimized pressure, the ion current was optimized to improve the index as well as packing density (fig.17). The optimized effect was achieved when the ion current density is 600 mA with the substrate temperature of 200 °C and oxygen pressure of 1.8×10^{-4} mbar. At lower ion currents, the negative inhomogeneity becomes dominant.

7.5 Ellipsometric Characterization

We have used the spectroscopic phase modulated ellipsometry (SPME) to analyze various optical properties of the ion-assisted films. For this the instrument used is Jobin-Yvon UVSEL-460 ellipsometer. As compared to other ellipsometric techniques like rotating analyzer ellipsometry (RAE), the phase modulation uses a high frequency modulation (50 kHz) provided by the photoelastic modulator. The SPME allows at least two orders of magnitude faster real-time measurements than RAE. Besides SPME introduces a wavelength dependent element, the photo acoustic modulator. Hence the this technique needs a very precise knowledge of the polarization of the light emerging from the modulator [32]. In the present work, the film parameters were fitted with three terms Sellemier formula. For some films multilayer approaches are used to fit experimental measurements.

In case of TiO_2 films the improved optical and structural properties were achieved at optimized ion beam parameters. It has been very consistently observed that there is a very intimate relationship amongst ion current, oxygen pressure and substrate temperature to achieve optimized refractive index (Figs21-24). As shown in the plot of refractive index, the highest index values were achieved at ion beam current of 650 mA with oxygen pressure and substrate temperature values at 1.8×10^{-4} mbar and 300 °C respectively (Fig.23). At this condition there is a degradation of index values with lower and higher ion currents. But as the pressure is increased, it is possible to achieve similar properties at a lower ion current (Fig.23). A typical experimental and theoretical ellipsometric fit is presented in Figs.21 & 24. The refractive index is fitted with Sellmier dispersion relation as follows:

$$n^2 = A + \frac{B\lambda^2}{(\lambda^2 - \lambda_0^2)} \qquad \ldots(8)$$

where, λ is the wavelength in nanometer, λ_0 is the wavelength of the oscillator.

At a relatively lower substrate temperature of 200 °C, oxygen pressure played a major role than ion current. In Fig.25 the variation of refractive index with respect to ion current is presented. The ellipsometric **Psi** and **Delta** parameters are depicted in Fig.26.

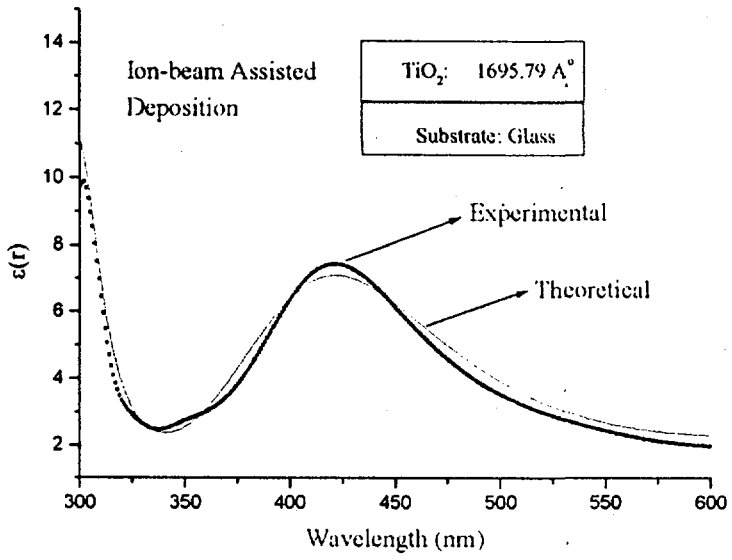

Fig.21 Fitting of theoretical ellipsometric data with experiments for TiO_2 film deposited with ion current 600 mA, O_2 pressure of $2x10^{-4}$mbar and Sub. Temp of 300 °C.

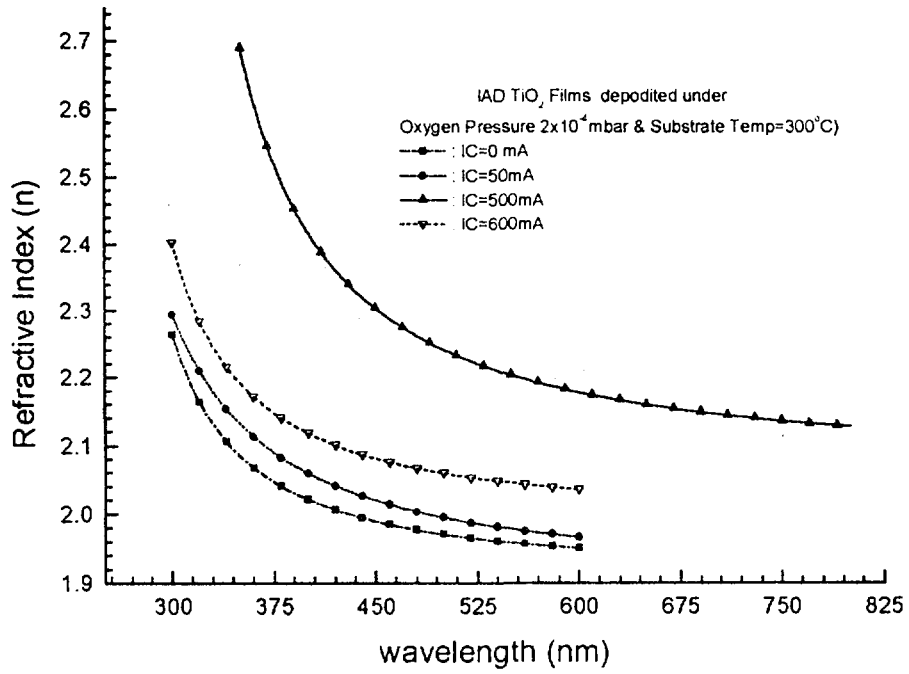

Fig.22 Spectral dependence of refractive indices of TiO_2 films deposited under same oxygen pressure and Temperature but with varying ion current.

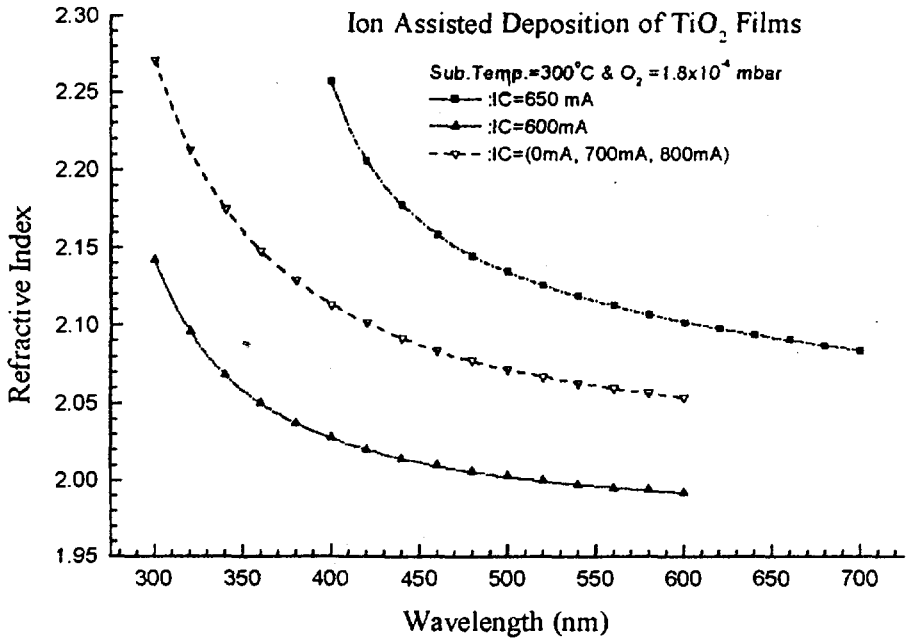

Fig.23 Spectral dependence of refractive indices of TiO_2 films deposited under optimized oxygen pressure (1.8x10^{-4} mbar) and Temperature but with varying ion current.

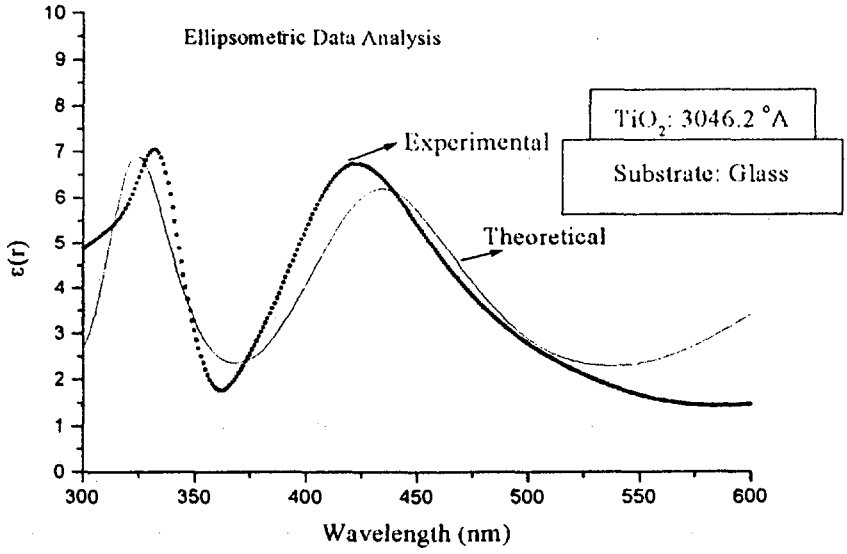

Fig.24 Fitting of theoretical ellipsometric data with experiments for TiO_2 film deposited with ion current 600 mA, optimized O_2 pressure of 1.8x10^{-4}mbar and Sub. Temp of 300 °C.

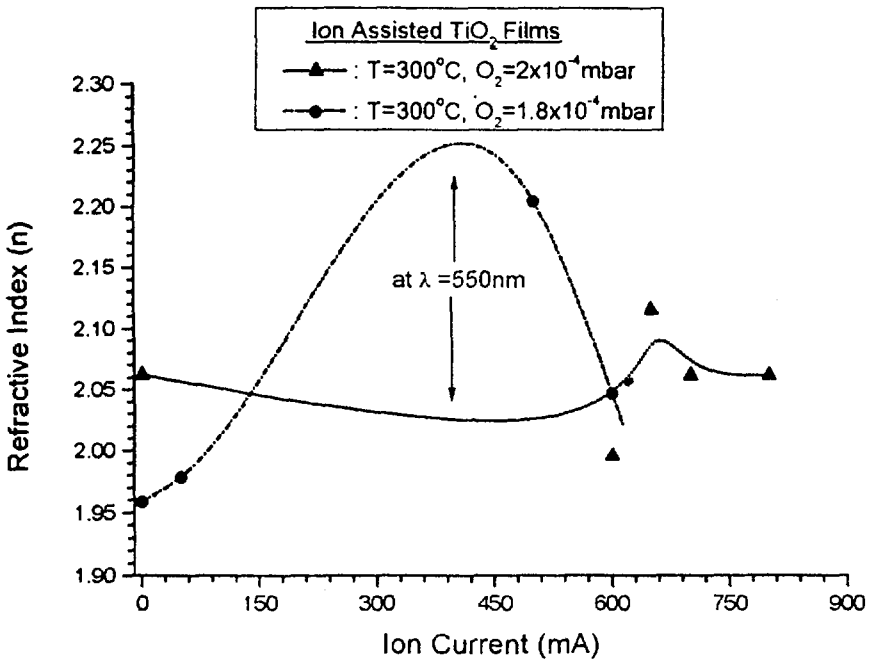

Fig.25 Variation of refractive index of IAD TiO_2 films with ion currents at two different Oxygen pressure.

As shown in Fig. 27, the highest refractive index has been achieved when the oxygen partial pressure was maintained at $1.5x10^{-4}$ mbar with ion current of 600 mA. But when the pressure is raised to $2.0x10^{-4}$ mbar the index decreased considerably. At this pressure the higher and lower ion current did not prove any advantageous for the refractive index. In Fig. 28 we have shown the quality of fitting between the experimental and theoretical data. Fig.29 shows the variation of refractive index with respect to oxygen pressure at this lower substrate temperature of 200 °C.

In case of ZrO_2 films, the ion current has a very interesting effect on the refractive index as shown in Fig.30. At lower and higher ion currents the index values improved but at intermittent points the index decreases. Fig.31 shows a typical fitting between theoretical and experimental ellipsometric measurements. In Fig.32, we have shown the effect ion currents at two different wavelength points. Unlike TiO_2 films, our experiments on ZrO_2 films have revealed that in later films, optical properties are invariably superior to the as-deposited condition.

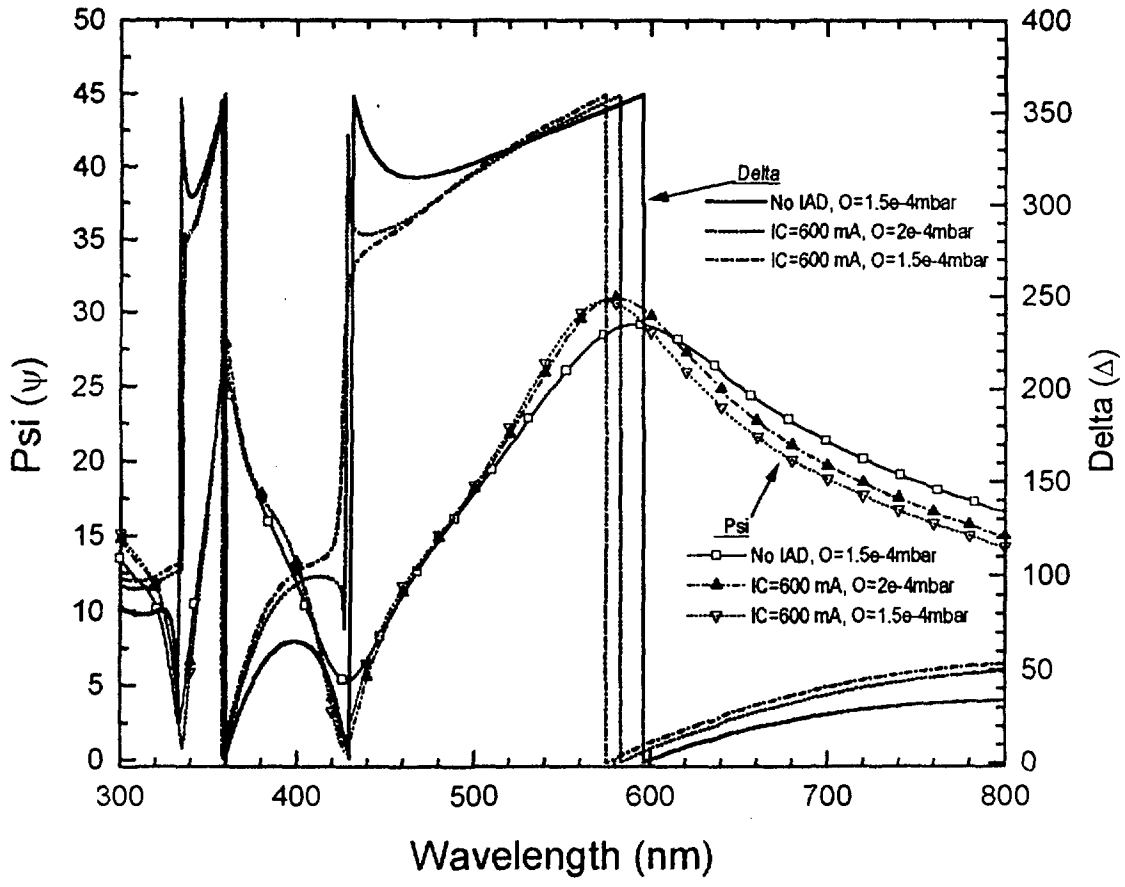

Fig.26 Ellipsometric measurements (Psi and Delta) of IAD films deposited at substrate temperature of 200 °C and various ion currents and oxygen pressures

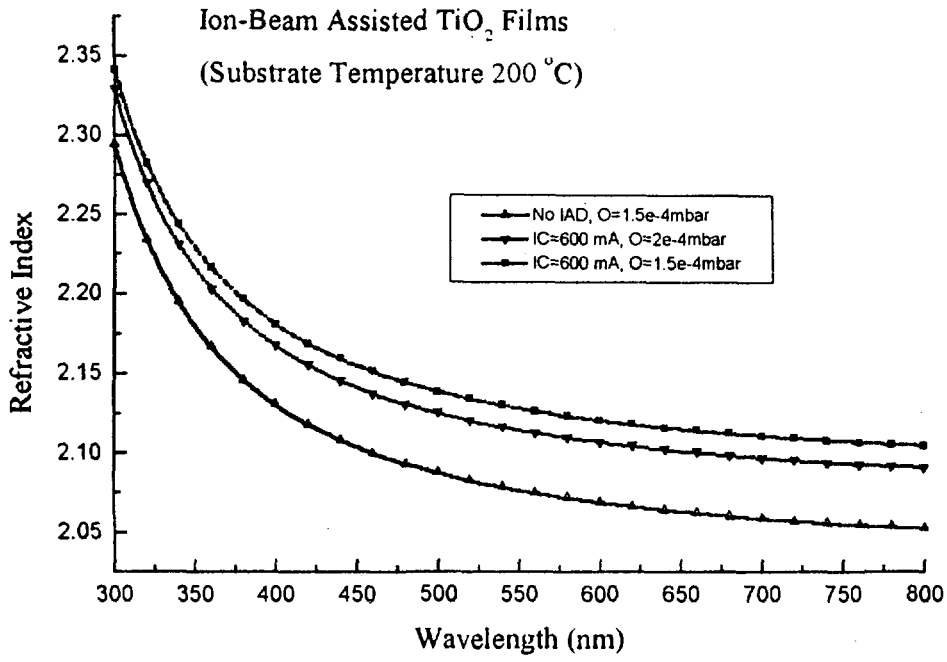

Fig.27 Refractive Index of IAD and Non-IAD TiO_2 Films

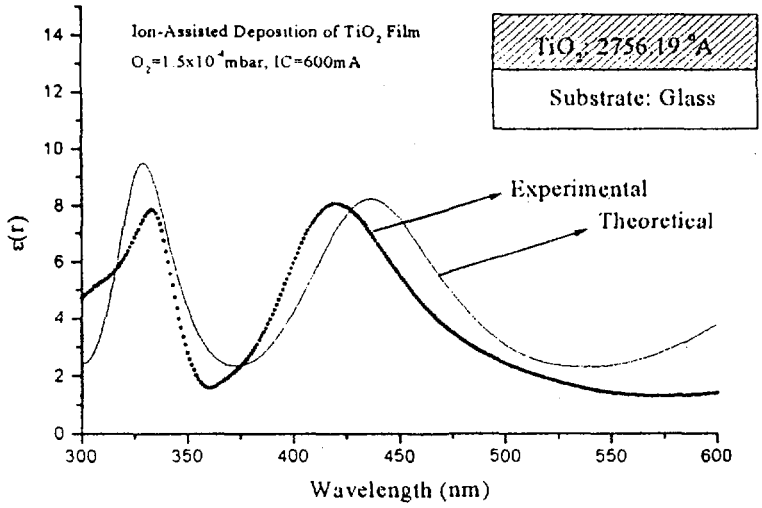

Fig.28 Fitting of theoretical ellipsometric data with experiments for TiO_2 film deposited with Ion current 600 mA, optimized O_2 pressure of $1.5x10^{-4}$mbar and Sub. Temp of 200 °C.

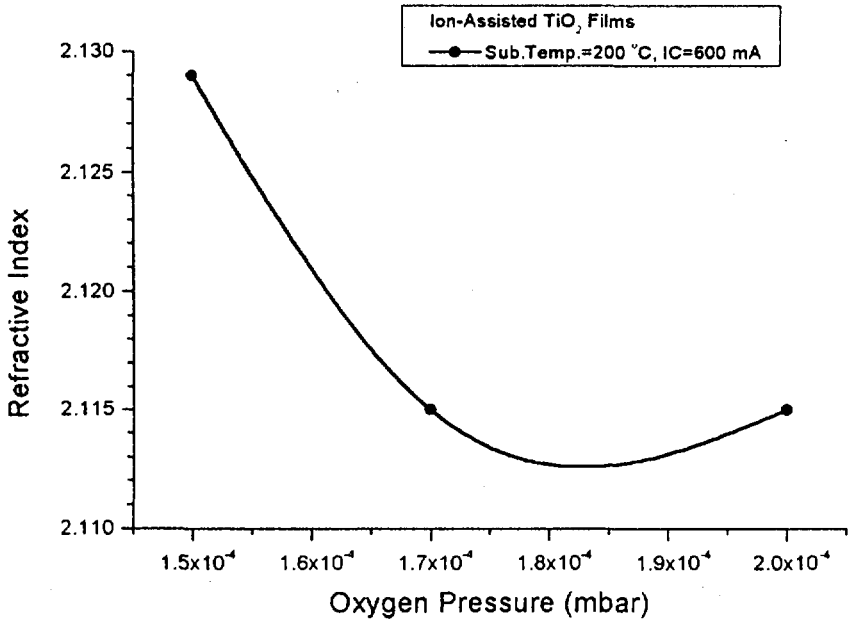

Fig.29 variation of refractive index of IAD TiO_2 films with respect to oxygen pressure

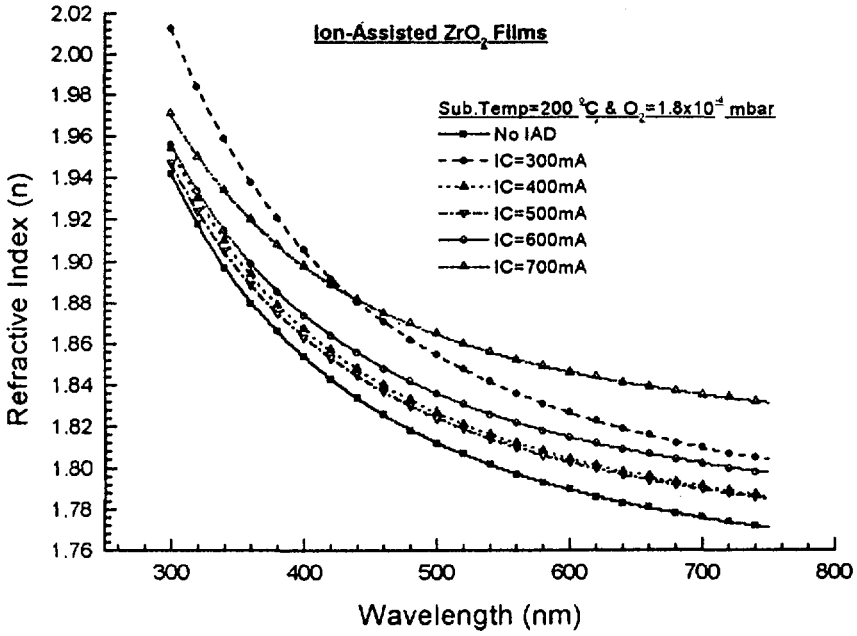

Fig.30 Spectral dependence of refractive indices of ZrO_2 films deposited under same oxygen pressure and Temperature but with varying ion current.

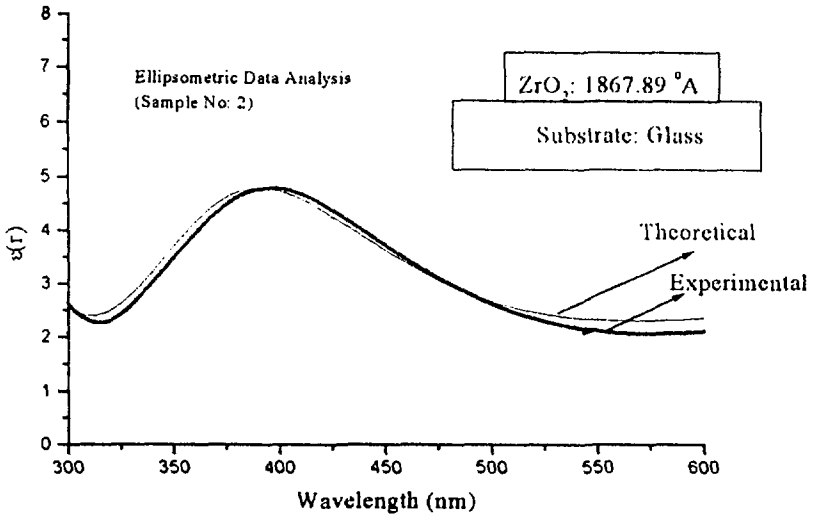

Fig.31 Fitting of theoretical ellipsometric data with experiments for ZrO_2 film deposited with Ion current 500 mA, optimized O_2 pressure of 1.8x10^{-4}mbar and Sub. Temp of 200 °C.

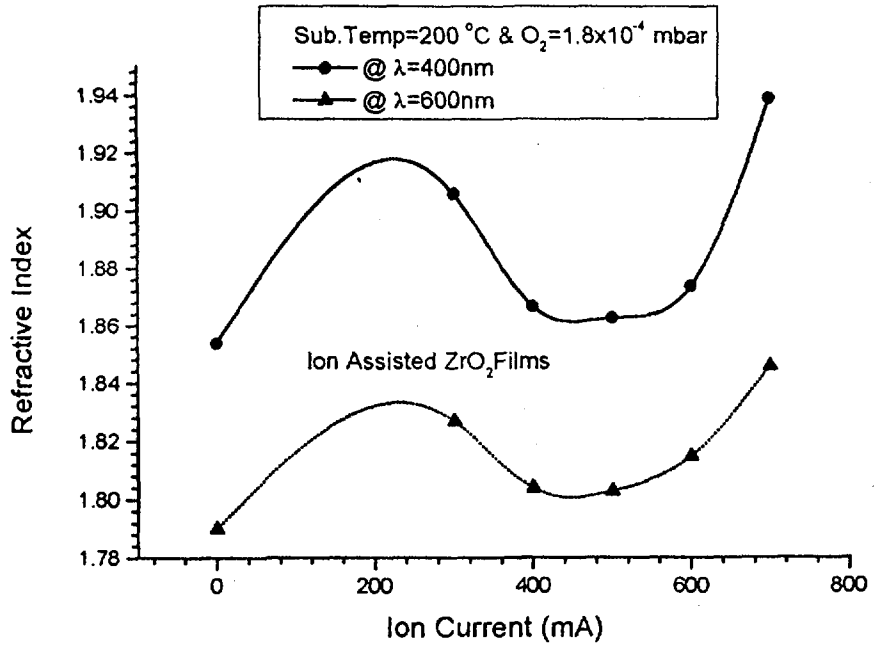

Fig.32 Variation of refractive index of IAD ZrO_2 films with ion currents at two different wavelengths.

8. Conclusion

In the present investigation, we have very successfully carried out ion assisted technique (IAD) to develop highly dense optical coatings for laser and spectroscopic applications. Various parameters of the ion gun as well as deposition system were optimized to achieve the best out of the process. Two of the very widely used refractory oxide materials, namely ZrO_2 and TiO_2 have been successfully optimized for the optimum index and homogeneity. Several all-dielectric multilayer devices have been developed using such IAD optimized films.

9. Acknowledgement

The authors convey their sincere thanks to Dr. A.P. Roy, Head Spectroscopy Division, for showing his keen interest and constant support for the work presented in this report.

Reference:

1. N.K. Sahoo and A.P. Shapiro, Appl. Opt., 37, 698 (1998)
2. M. Harris, H.A. Macleod, S. Ogura, E. Pelletier and B. Vidal, Thin Solid films, 57, 173 (1979)
3. W.C. Herrman and J.R. McNeil, Proc.Soc.Photo-Opt. Instrum. Eng. (SPIE), 325, 101 (1982)
4. G. Carter and D.G. Armour, Thin Solid Films, 80, 13 (1981)
5. K.H. Muller, J. Vac. Sci. Technol A, 4, 184 (1986)
6. K.H. Muller, R.P. Netterfield and P.J. Martin, Phys. Rev. B, 35, 2934 (1987)
7. S. Mohan and M. Ghanashyam Krishna, Vacuum, 46, 645 (1995) (and references therein)
8. D. Dobrev and M. Marinov, Cr Acad Bulg Sci., 26, 231 (1973)
9. V.O. Babnev, Ju V. Bykov and M.B. Guseva, Thin Solid Films, 38, 1 (1976)
10. P.J. Martin and R.P. Netterfield, Appl. Opt., 24, 1732 (1985)
11. J.J. McNally, PhD Thesis, "Ion assisted deposition of optical coatings", (University of New Mexico, 1986)
12. R.P. Netterfield, W.G. Sainty, P.J. Martin and S.H. Sie, Appl. Opt., 24, 2267 (1985)
13. P.J. Martin, R.P. Netterfield and W.G. Sainy, J. appl. Phys., 55, 235 (1984)
14. J.R. MacNeil, A.C. Barron, S.R. Wilson and W.C. Hermann Jr., Appl. Opt., 23, 552 (1984)
15. P.J. Martin and R.P. Netterfield, Optical films produced by ion based techniques, in progress in Optics, edited by E. Wolf, (North Holland, New York), 23, 115 (1986)
16. P.J. Martin. J. Matter. Sci., 21, 1 (1986)
17. A.S. Kao and G.L. Gorman, J. appl. Phys., 67, 3826 (1990)
18. H.F. Winters and P. Sigmund, J. Appl. Phys., 45, 4760 (1974)
19. H.R. Kaufman, J.J. Cuomo and J.M.E. Harper, J. Vac. Sci. Technol., 21, 725 (1982)
20. J. Ebert Proc.Soc.Photo-Opt. Instrum. Eng. (SPIE), 325, 29 (1982)
21. R.S. Robinson and H.R. Kaufman, Hand Book of Ion Beam Technology, p221, J.J. Cuomo, S.M. Rossnagel and H.R. Kaufman (Eds.) Noyes, New Jersey (1989)
22. P.R. Denton and A. Musset, Proc. Soc. Vac. Coaters, 27th Tech. Conf., p76 (1984)
23. H.R. Kaufman, Adv. Electron. Phys, 36, 265 (1974)

24. R.G. Wilson, and G.R. Brewer, "Ion Beams with Application to Ion Implantation", Wiley, New York, p100 (1973)
25. J.A. Dobrowolski, F.C. Ho, D. Megnagh, R. Simpson and A. Waldorf, Appl. Opt. 26, 5204 (1987)
26. B.A. Movchan and A.V. Demchishin, Fiz.Met.Metalloved., 28, 653 (1969)
27. J.M. Pearson, Thin Solid Films, 6, 349 (1970)
28. E.H. Hirsch and K.I. Varga, Thin Solid Films, 52, 445 (1978)
29. D.R. Brighton and G.K. Hubler, Nucl. Instrum. Meth. In Phys. Resch.B, 28, 527 (1987)
30. G.I. Grigorov, I.N. Martev, J.P. Langeron and J.L. Vignes, Thin Solid Films, 161, 249 (1988)
31. N.K. Sahoo and K.V.S.R. Apparao, Appl. Phys. A, 63, 195 (1996)
32. B. Drevillon, J.Y. Parey and M. Stchakovsky, Proc.Soc.Photo-Opt. Instrum. Eng. (SPIE), 1188, 174 (1989)

Published by : Dr. M. R. Balakrishnan, Head Library & Information Services Division
Bhabha Atomic Research Centre, Mumbai - 400 085, INDIA.